Transonic Full Potential Solutions by an Integral Equation Method

K. S. Ravichandran,* N. L. Arora,† and R. Singh‡
Indian Institute of Technology, Kanpur, India

A hybrid computational procedure combining the integral equation method with elements of finite difference techniques is developed to obtain two-dimensional transonic flow solutions with embedded shocks to the full potential equation at subsonic freestream Mach numbers. Integral equations for the perturbation velocity components are formulated in terms of an internal singularity distribution and a nonlinear field source distribution representing compressibility effects. For supercritical flows the field source term is augmented by the addition of an artificial viscosity term. Derivative computations are carried out on a transformed plane using finite difference formulas and physical plane derivatives obtained using the Jacobian of the transformation. A simple direct iteration scheme is employed for the numerical solution of the integral equations for the velocity field. Surface pressure distributions obtained for subcritical as well as supercritical cases compare favorably with earlier results.

I. Introduction

TRANSONIC flow solutions to the full potential equation (FPE) have been obtained by numerous researchers using finite difference,[1-3] finite volume,[4] and finite-element[5] techniques for a wide class of flows and body geometries. However, although the integral equation method (IEM) is one of the oldest methods used for calculating transonic flows, the use of the shock-capturing field panel technique for the computation of supercritical flows with shocks has been restricted thus far to thin airfoils and slender bodies based on the small-disturbance theory.[6,7] Spreiter[8] has given a recent review of the IEM as applied to small-perturbation transonic flow computations. A few successful attempts have been made earlier to compute full potential subcritical solutions using the IEM by Luu et al.[9] and Stricker[10] (the authors are aware of the elements of the latter work only reported by Kraus[11]). Using Green's theorem, Stricker obtains an integral equation for the velocity potential in terms of the surface distribution of sources and vortices and a field integral representing the compressibility effects. A discretization technique based on the field panel method yields the velocities and their derivatives for each control point in terms of sum formulas replacing the integrals. The Kutta condition is satisfied at every iteration by setting the transverse velocity component at the trailing edge to zero. Results obtained for subcritical flows over a NACA 0012 airfoil agree well with test cases given by Lock.[12]

In the present work, a hybrid calculation procedure combining the IEM with elements of the finite difference technique is adopted to compute full potential solutions to two-dimensional transonic flows over airfoils with large embedded supersonic regions and comparatively strong shocks.

The present approach differs from Stricker's in the sense that 1) the singularities, instead of being distributed on the surface, are distributed internally along the mean line of the airfoil as was done by Basu[13] for incompressible flows; and 2) the derivatives are calculated using finite difference formulas, thus enabling the introduction of artificial viscosity and upwind differencing for the computation of supercritical flows. For comparable accuracy, the use of internal singularities involves fewer unknowns as compared to the surface singularity model. This leads to a very substantial reduction in the memory requirements for implementing the IEM for compressible full potential calculations because the IEM requires a large number of influence coefficients to be calculated and stored. Also, the use of internal singularities does away with the need for surface paneling so that the tangency boundary condition on the body surface is satisfied more accurately.

For compressible flow computations, a field source distribution, which is a function of the velocities and their derivatives, is involved in addition to the internal singularities. The velocity derivatives could be obtained directly on the physical plane using a Cartesian mesh, but for reasons discussed in Sec. III, a body-conforming mesh is preferred. The mesh is generated by a sequence of coordinate transformations given by Mercer et al.[14] The derivative calculations are carried out on the transformed plane and the physical plane derivatives are obtained using the Jacobian of the transformation.

The field source distribution is computed at each step of an iterative procedure, resulting in additional induced velocities that disturb the tangency boundary condition on the body surface. The internal singularity distribution is accordingly redetermined at every iteration in order to satisfy the tangency boundary condition. The nonlinear problem thus reduces at every iteration to a Poisson one.

For supercritical flows with embedded shocks at subsonic freestream Mach numbers, the field source term is augmented by an artificial viscosity term in the supersonic region to exclude expansion discontinuities and to replace compression shocks by continuous narrow regions of large velocity gradients. The artificial viscosity term is modeled after Jameson's rotated difference scheme[15] to insure the correct domain of dependence for flows with large embedded supersonic zones.

Calculations have been carried out for two test airfoils NACA 0012 and NACA 64A410 at subcritical and supercritical Mach numbers. The results are comapred with those obtained by other methods.

II. Problem Formulation

The Inviscid Equations

A Cartesian coordinate system with origin at the leading edge and x axis aligned with the chord of the airfoil is selected. Steady, inviscid, irrotational, compressible, two-dimensional

Received Nov. 16, 1982; revision received July 28, 1983.

*Graduate Student, Department of Mechanical Engineering.
†Professor, Department of Aeronautical Engineering (presently Visiting Professor, Department of Mechanical and Aeronautical Engineering, Carleton University, Ottawa, Canada).
‡Assistant Professor, Department of Mechanical Engineering.

flow past arbitrary bodies is completely described by the equation of continuity

$$\frac{\partial}{\partial x}(\rho\Phi_x)+\frac{\partial}{\partial y}(\rho\Phi_y)=0 \tag{1}$$

and the energy equation

$$c^2+[(\gamma-1)/2]Q^2=1/M_\infty^2+(\gamma-1)/2 \tag{2}$$

where Φ is the velocity potential, Q the fluid speed, c the local speed of sound, ρ the density, M_∞ the freestream Mach number, and γ the ratio of specific heats.

It is convenient to work in terms of the perturbation potential. The total potential can then be expressed as

$$\Phi=x\cos\alpha+y\sin\alpha+\phi \tag{3}$$

where ϕ is the perturbation potential and α the angle of attack. The speed is given by

$$Q^2=(\cos\alpha+u)^2+(\sin\alpha+v)^2 \tag{4}$$

where u and v are the perturbation components. Equations (1) and (2) must be supplemented by the isentropic relations between the pressure, density, and speed of sound

$$p=\rho^\gamma, \qquad c^2M_\infty^2=\rho^{\gamma-1} \tag{5}$$

In Eqs. (1-5) all velocities have been referred to the freestream velocity, while the pressure and density are referred to their respective freestream values. In terms of the perturbation potential, Eq. (1) together with Eqs. (2) and (5) yields the quasilinear equation

$$\phi_{xx}+\phi_{yy}=\frac{Q}{c^2}\frac{\partial}{\partial s}\left(\frac{Q^2}{2}\right)\equiv g \tag{6}$$

where $\partial/\partial s$ denotes the derivative along a streamline.

If the airfoil shape is prescribed as $y=F(x)$, $0\le x\le 1$, the tangency condition can be expressed in terms of the perturbation velocity components as

$$v-F'(x)u=\cos\alpha F'(x)-\sin\alpha \text{ on } y=F(x) \tag{7}$$

The far-field condition is expressed as

$$u,v\to 0 \text{ as } (x^2+y^2)^{1/2}\to\infty \tag{8}$$

In addition, the Kutta condition of smooth flow must be satisfied at the trailing edge for a unique solution.

Artificial Viscosity

For purely subcritical flows, Eqs. (2-8) together with the Kutta condition uniquely determines the solution for the flow past an airfoil. When the flow becomes supercritical, shocks may appear in the solution and the directional property corresponding to the entropy inequality must be introduced in order to exclude expansion shocks and capture only compression shocks. For the treatment of flows with large supersonic zones, the direction of upwind differencing is not known in advance. Following Jameson,[15] this difficulty is overcome by the introduction of an auxiliary coordinate system that is locally aligned with the flow direction. If s and n represent the streamwise and normal directions, respectively, then Eq. (6) can be written as

$$(c^2-Q^2)\Phi_{ss}+c^2\Phi_{nn}=0 \tag{9}$$

Now upwind differencing of Φ_{ss} at supersonic points has the correct domain of dependence and results in an artificial viscosity

$$T=-\Delta s\mu Q^2\Phi_{sss} \tag{10}$$

where μ is the switching function defined by

$$\mu=\max\{0,[1-(c^2/Q^2)]\}$$

For the integral equation formulation, an artificial viscosity term corresponding to Eq. (10) may be explicitly added to the field source term. Since the mass continuity equation is equivalent to multiplying Eq. (6) by ρ/c^2, the conservation form of the artificial viscosity term may be approximated as

$$T\simeq-\frac{\partial}{\partial s}\left[\Delta s\mu\frac{\rho}{c^2}Q\frac{\partial}{\partial s}\left(\frac{Q^2}{2}\right)\right] \tag{11}$$

With the addition of artificial viscosity, the field source term

$$\bar{g}=g+T \tag{12}$$

replaces g in Eq. (6).

Since the inviscid term in Eq. (12) is not in conservation form, whereas T is, solutions to Eq. (6) with $\bar{g}$ given by Eq. (8) may be termed as quasiconservative. Further, note that since the field source term in Eq. (6) can also be expressed as $-(Q/\rho)(\partial\rho/\partial s)$, artificial compressibility may be easily introduced by replacing the density ρ with a modified density $\tilde{\rho}$.[16] In the present paper, however, results of computations using only artificial viscosity will be presented.

The Integral Equation

The equation for the perturbation potential ϕ may be regarded as a Poisson equation with the nonlinear term $\bar{g}$ acting as a field source distribution. The solution for ϕ may therefore be expressed as the sum of a general solution satisfying the homogeneous equation and a particular solution.

Since the general solution satisfies the Laplace equation, it can be built up by a suitable distribution of singularities. See Fig. 1. For two-dimensional lifting flows, a combination of source and vortex distributions may be assumed on the airfoil surface (surface singularities) or on the mean line (internal singularities). Adopting the latter model, the potential induced at a field point (x,y) may be expressed as the sum of the potentials induced by the internal singularities and the field source $\bar{g}$. Therefore,

$$\phi(x,y)=\int_C K_s[x-\xi,y-y_m(\xi)]\sigma[\xi,y_m(\xi)]\,d\xi + \int_C K_v[x-\xi,y-y_m(\xi)]\gamma[\xi,y_m(\xi)]\,d\xi + \iint_D K_s(x-\xi,y-\eta)\bar{g}(\xi,\eta)\,d\xi\,d\eta \tag{13}$$

In Eq. (13), σ and γ represent the source and vortex distributions, respectively, along curve C, which denotes the mean line $y=y_m(x)$. The kernels K_s and K_v are those for a two-dimensional source and vortex, respectively, and are given by

$$K_s(x-\xi,y-\eta)=\frac{1}{2\pi}\ell n[(x-\xi)^2+(y-\eta)^2]^{1/2}$$

$$K_v(x-\xi,y-\eta)=\frac{1}{2\pi}\tan^{-1}\frac{y-\eta}{x-\xi}$$

and D denotes the entire x-y plane, excluding the area enclosed by the airfoil.

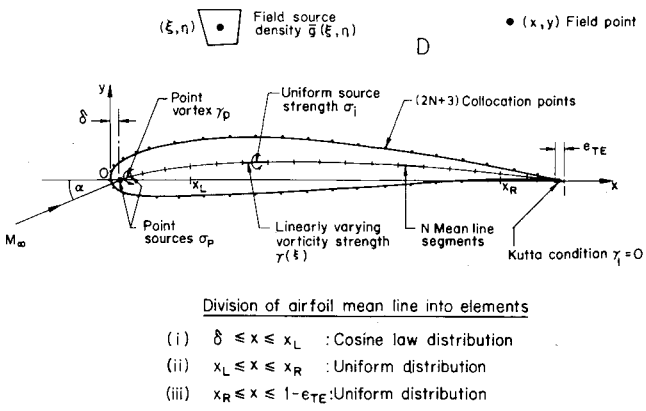

Fig. 1 Singularity model for airfoil in compressible flow and location of the collocation points.

The integral equations for the perturbation velocity components may be obtained by differentiating Eq. (13) with respect to x and y. Adopting the functional notation for brevity,

$$\phi(x,y) = \mathfrak{IC}(K_s, K_v)$$

$$u(x,y) = \mathfrak{IC}(K_{sx}, K_{vx}) \tag{14}$$

$$v(x,y) = \mathfrak{IC}(K_{sy}, K_{vy}) \tag{15}$$

Equations (14) and (15) represent a system of two simultaneous nonlinear integral equations for u and v that must be solved subject to the boundary conditions [Eqs. (7) and (8)] and the Kutta condition. It is easily seen that the far-field condition is implicitly satisfied by Eqs. (14) and (15) if, for the field integral, we make appropriate assumptions about the asymptotic behavior of $\bar{g}$.

III. Numerical Solution

Grid Generation

It is possible to discretize the system of Eqs. (7), (14), and (15) on the physical plane using rectangular panels with sides parallel to the coordinate axes. The drawback of this procedure is that the special care necessary to cluster the mesh cells in the leading edge region makes the grid construction airfoil dependent and complicates input data specification. Moreover, such a mesh leads to uneconomic storage and inefficient coding, especially for lifting flows. A curvilinear grid generated through well-defined analytical/numerical transformations does away with these difficulties. Thus, the following sequence of transformations is defined to construct the transformed ν-θ plane from the physical plane[14]:

$$\bar{x} = x - r_t \qquad \bar{y} = y \tag{16a}$$

$$s + it = \cosh^{-1}(1 - 2e^{\bar{x}+i\bar{y}}) \tag{16b}$$

$$\nu = s \qquad \theta = t/t_{\text{upper}} \tag{16c}$$

where r_t is the leading-edge radius for round-nosed airfoils or a small positive value for sharp-nosed airfoils. The last transformation yields a rectangular domain in which the upper and lower surfaces of the airfoils are stretched into $\theta = 1$ lines on either side of the θ axis. The upstream infinity maps onto the origin of the ν-θ plane. The downstream infinities of the upper and lower surface wakes on the physical plane correspond, respectively, to the negative and positive infinities of the ν axis.

The rectangular domain on the ν-θ plane is divided into smaller rectangular cells (Fig. 2). This rectangular grid is now mapped back to the physical plane, yielding constant ν-θ lines

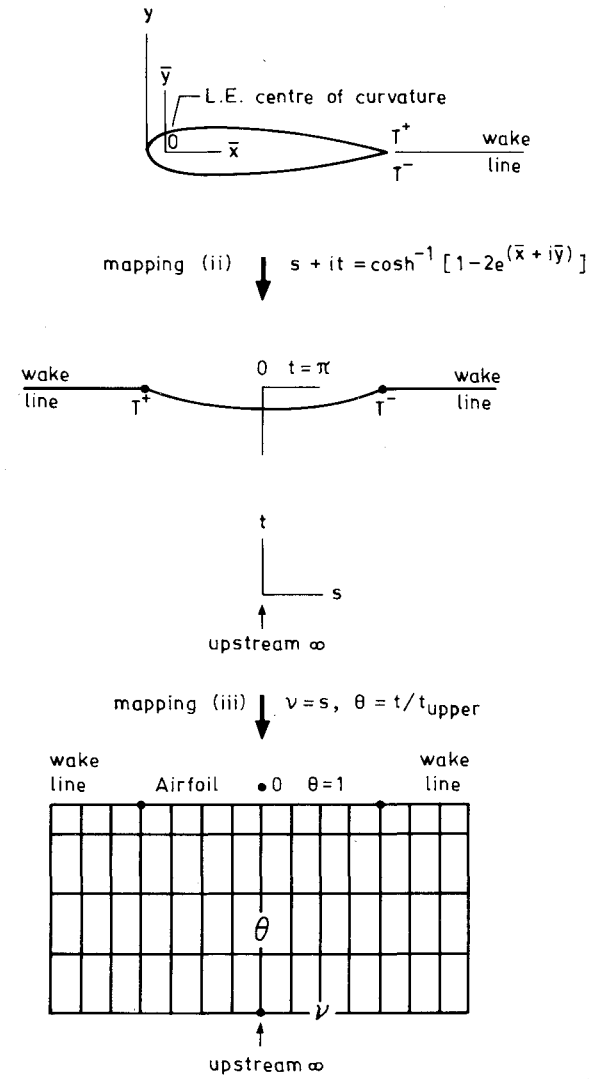

Fig. 2 Grid generation through coordinate transformations.

that constitute the curvilinear grid on the latter plane (Fig. 3). All of the derivatives are computed on the ν-θ plane by finite differences and derivatives on the physical plane are obtained using the Jacobian of the transformation, according to the formula

$$J\left[\frac{\partial}{\partial \nu}, \frac{\partial}{\partial \theta}\right]^T = \left[\frac{\partial}{\partial x}, \frac{\partial}{\partial y}\right]^T \tag{17}$$

where J, the Jacobian, is given by

$$J = \begin{bmatrix} \dfrac{\partial \nu}{\partial x} & \dfrac{\partial \nu}{\partial y} \\ \dfrac{\partial \theta}{\partial x} & \dfrac{\partial \theta}{\partial y} \end{bmatrix}$$

Discretization

Equations (14) and (15) will now be discretized by replacing the integrals with sums and derivatives by finite differences. Figure 1 shows the discretization of the mean line and the location of the collocation points on the airfoil surface. A small gap δ is maintained between the leading edge of the airfoil and the segment of the chord nearest to it to avoid infinite velocities near the leading edge. The interval

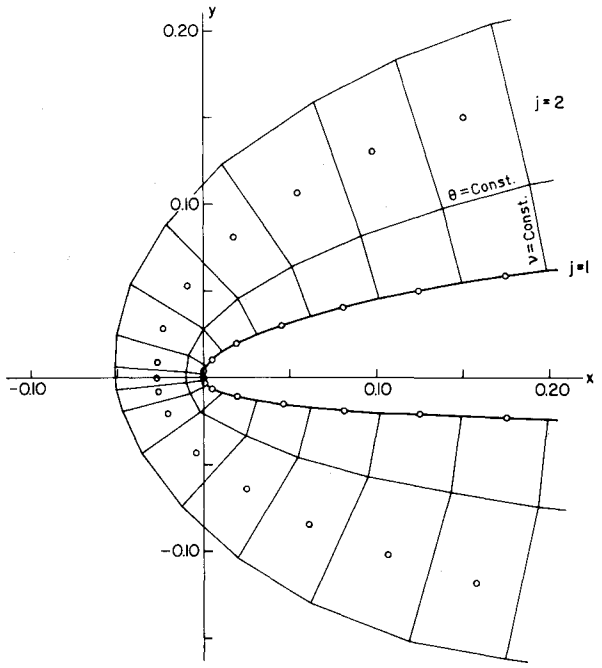

Fig. 3 Section of the grid on the physical plane.

$x_L \le x \le x_R$ denotes the anticipated extent of the supersonic zone for a supercritical case.

On each element of the discretized mean line, the source strength is assumed to be uniform, while the vorticity is assumed to have a linear variation. Following Basu,[13] two point sources are placed at either end of the mean line element nearest to the leading edge, while one point vortex is placed at the midpoint of the same element (Fig. 1). Expressions for the influence coefficients of the internal singularities may be found in Ref. 13 and will not be given here for reasons of space.

When the mean line is divided into N segments, we have $2N+4$ unknown singularity strengths to be determined. This implies that the tangency condition must be satisfied at $2N+3$ collocation points, yielding as many equations, with the remaining equation necessary for a unique solution obtained from the Kutta condition, which in the present method is satisfied by setting the vorticity strength to zero at the trailing edge.

In a particular calculation the value of N is initially fixed. If N_w denotes the number of points chosen beyond the trailing edge and if index i runs from 1 to n and index J from 1 to m, the total number of field panels is given by $n \times m = 2m(N+N_w)+3m$.

The field integrals in Eq. (15) may now be replaced by summations. In each cell formed by the intersection of constant ν and θ lines on the physical plane, all of the flow variables are considered to be uniform. Each cell is approximated by a quadrilateral and its influence coefficient at every field point is evaluated analytically following a method outlined by Hess.[17]

Denoting with subscript I the velocities induced by the internal singularities and with subscript F those due to the field sources, the discretized equations may be written as

$$u = u_I + u_F \tag{18}$$

$$v = v_I + v_F \tag{19}$$

$$u_I(x,y) = \sum_{k=1}^{N+2} a^k(x,y)\,\sigma_k + \sum_{k=1}^{N+2} c^k(x,y)\,\gamma_k \tag{20}$$

$$v_I(x,y) = \sum_{k=1}^{N+2} b^k(x,y)\,\sigma_k + \sum_{k=1}^{N+2} d^k(x,y)\,\gamma_k \tag{21}$$

$$u_F(x,y) = \sum_{l}\sum_{k} e^{kl}(x,y)\,\bar{g}_{kl} \tag{22}$$

$$v_F(x,y) = \sum_{l}\sum_{k} f^{kl}(x,y)\,\bar{g}_{kl} \tag{23}$$

where a, b, c, and d denote the influence coefficients for the internal singularities, while e and f denote those for the field sources. Note that the contributions from the point sources and the point vortex have been absorbed in the vectors σ and γ, respectively.

Inserting Eqs. (18) and (19) in Eq. (7), we obtain the following equation for the tangency boundary condition,

$$v_I - F'(x)\,u_I = F'(x)\cos\alpha - \sin\alpha + F'(x)\,u_F - v_F$$

$$\text{on } y = F(x) \tag{24}$$

In matrix form, Eq. (24) is written as

$$C_{ik}\left[\{\sigma_k\}\{\gamma_k\}\right]^T = [N_i]^T + [h_i]^T \tag{25}$$

where

$$N_i = F'(x_i)\cos\alpha - \sin\alpha \tag{26}$$

$$h_i = F'(x_i)\,u_F(x_i,y_i) - v_F(x_i,y_i) \tag{27}$$

and (x_i,y_i) denote the collocation points on the airfoil surface.

The vector h_i arises because of the presence of the nonlinear term. Setting $h_i = 0$ gives the solution for incompressible flow. The matrix C, embodying the tangency boundary condition on the airfoil surface, remains fixed throughout the iterative procedure.

Calculation of $\bar{g}$

The field source term [Eq. (12)] consists of an inviscid term and an artificial viscosity term. The inviscid part may be evaluated as

$$g = \frac{Q}{c^2}\frac{\partial}{\partial s}\left(\frac{Q^2}{2}\right) = \frac{U}{c^2}(Uu_x + Vv_x) + \frac{V}{c^2}(Uu_y + Vv_y) \tag{28}$$

Now if u_x and u_y are known, using the governing equation and the irrotationality condition,

$$v_y = \bar{g}^{\text{old}} - u_x \quad \text{and} \quad v_x = u_y \tag{29}$$

The derivatives of u are computed on the ν-θ plane using second-order central differences at interior points and one-sided differences at boundary points. The physical plane derivatives are obtained using Eqs. (17).

For the artificial viscosity term, assuming that the streamlines do not deviate much from the ν coordinate lines in the supersonic regions for the airfoils to be considered, one may use upwind differencing directly on the physical plane. Hence,

$$T_{ij} = G_{ij} - G_{i+1,j} \quad \text{on the upper surface}$$

$$= G_{ij} - G_{i-1,j} \quad \text{on the lower surface} \tag{30}$$

where

$$G = -\mu\frac{\rho}{c^2}Q\frac{\partial}{\partial s}\left(\frac{Q^2}{2}\right)$$

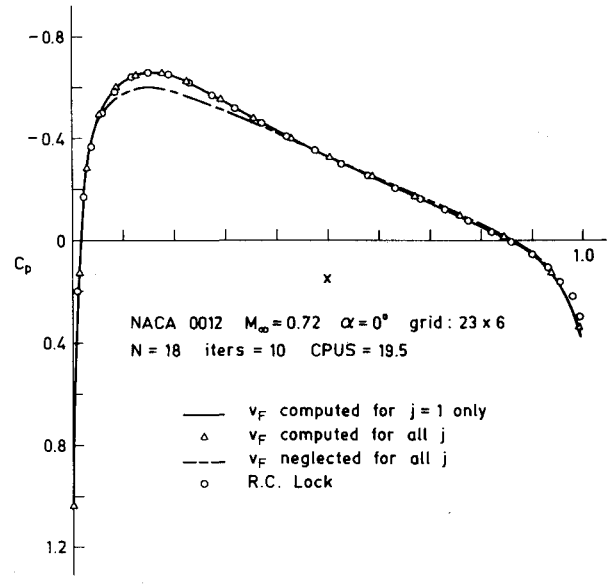

Fig. 4 Effect of neglecting nonlinear contribution v_F to the v component of velocity.

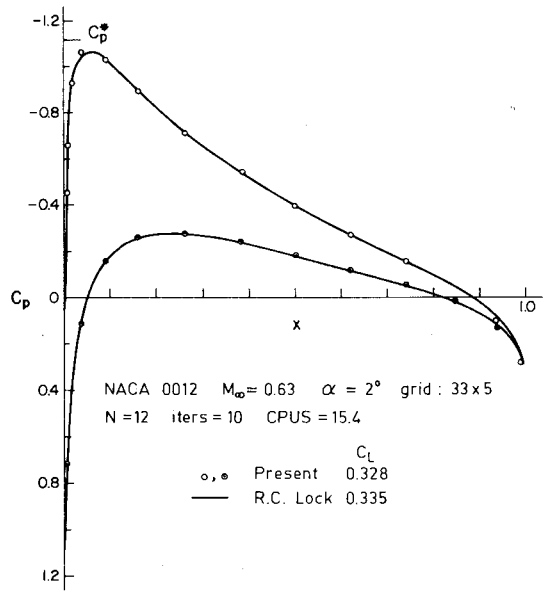

Fig. 5 Subcritical pressure distribution over NACA 0012 airfoil at incidence.

In actual calculations, the artificial viscosity calculated from Eq. (30) was found to produce too little dissipation to achieve convergence of strong supercritical flows. Hence, the switching function μ in Eq. (30) is replaced by $\lambda\mu$, where $\lambda \geq 1$ is an artificial viscosity parameter. λ provides a simple means of controlling the magnitude of dissipation for a given case and hence the stability of the iteration scheme.

For $j=1$, the velocities computed using Eqs. (18) and (19) give the surface values because the influence coefficients of the field panels adjacent to the body surface represent induced velocities at the collocation points located on the surface of the airfoil. These are required for satisfying the tangency boundary condition. The representative field strength $\tilde{g}$ for each of these source panels is computed from the velocities and their derivatives at the collocation points and represents the values at points located at the edge of the panel rather than in the interior, as is the case for panels $j \geq 2$ (see Fig. 3). Actual calculations show that good comparison with the finite difference conservative results is achieved with such an approximation for $\tilde{g}$.

Iterative Procedure

A simple direct iteration scheme is used to solve Eqs. (18) and (19) for the unknown velocity field. For a purely subsonic case, the scheme represents an incompressible linear operator that, by repeatedly acting on a nonlinear forcing term to satisfy the surface boundary condition, produces quick convergence in the entire flowfield in about 15 iterations or less. For supercritical cases with the introduction of artificial viscosity, it is found that convergence can be achieved with the same scheme even for flowfields with fairly large embedded supersonic zones, without the addition of artificial time-dependent damping terms. However, to insure stability of the iteration scheme for strong supercritical cases, a term $\alpha_t u_t$ was added to the field source term $\tilde{g}$.

If the estimate $\tilde{g}^{(n)}$ is available at the nth iteration, we obtain two simple linear integral equations for the singularity strengths σ and γ that are determined by satisfying the tangency condition prescribed by Eq. (7). The field source term is now recalculated and this procedure is repeated until convergence is obtained in the entire flowfield. The initial estimate of $\tilde{g}$ for the present calculations was obtained from the incompressible flow solution. The convergence criterion was specified in terms of maximum change in the value of the field source distribution. In the following calculations, the iterative procedure was terminated when $\max_{i,j} |\Delta \tilde{g}| \leq 0.005$.

Instead of the present incompressible operator, the use of a compressible operator was also considered. This would probably have given a better initial estimate of $\tilde{g}$. However, its use would have made the grid construction and hence the influence coefficient calculation dependent upon the freestream Mach number, necessitating their computation whenever M_∞ is changed.

IV. Results and Discussion

The above numerical procedure has been coded in FORTRAN and run on a DEC-1090 computer. Test runs have been carried out using a NACA 0012 airfoil for which subcritical and supercritical results are available for comparison. Subcritical results are compared with test cases given by Lock[12] and supercritical comparisons are made with the quasiconservative results given in Ref. 18.

Before presenting the main results, an approximation made in the calculation of the nonlinear contribution to the v component of the velocity [Eq. (23)] will be discussed. In an attempt to economize on storage requirements, it was found through numerical experiments that it is sufficient to calculate this contribution for only the $j=1$ level on the surface. The effect of this approximation on the surface pressure distribution for symmetric subcritical flow past a NACA 0012 airfoil at $M_\infty = 0.72$ is shown in Fig. 4. It is seen that the results obtained using the above approximation agree well with those obtained without such an approximation and both are in good agreement with the results of Lock.[12] Although no such tests were carried out for supercritical cases, it is believed that for the relatively thin and low cambered airfoils for which computations were carried out, the above approximation does not cause significant errors in the resulting pressure distributions. All of the results that follow were obtained incorporating the above approximation in the computer code.

Figure 5 shows the computed pressure distribution over a NACA 0012 airfoil for a subcritical lifting case with $M_\infty = 0.63$ and $\alpha = 2$ deg. The results are compared with those given by Lock.[12] It is seen that the agreement between the two results is good everywhere except for small discrepancies in the region of the velocity peak near the leading edge. The computed lift coefficient differs by only about 3% from the value given by Lock. It is noted that there is a slight

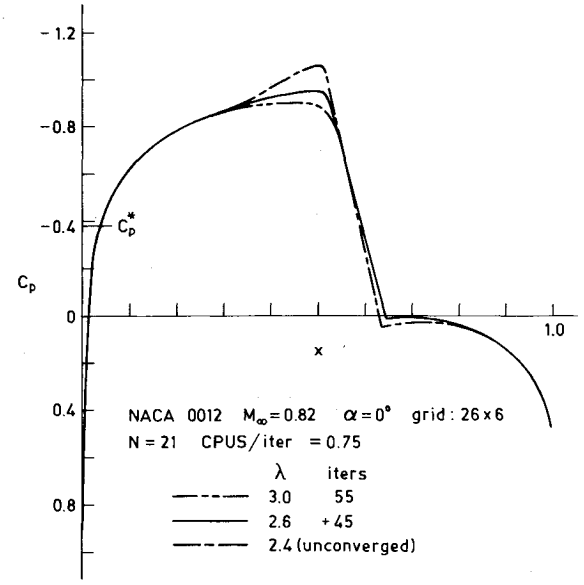

Fig. 6 Effect of λ on the surface pressure distribution for a NACA 0012 airfoil.

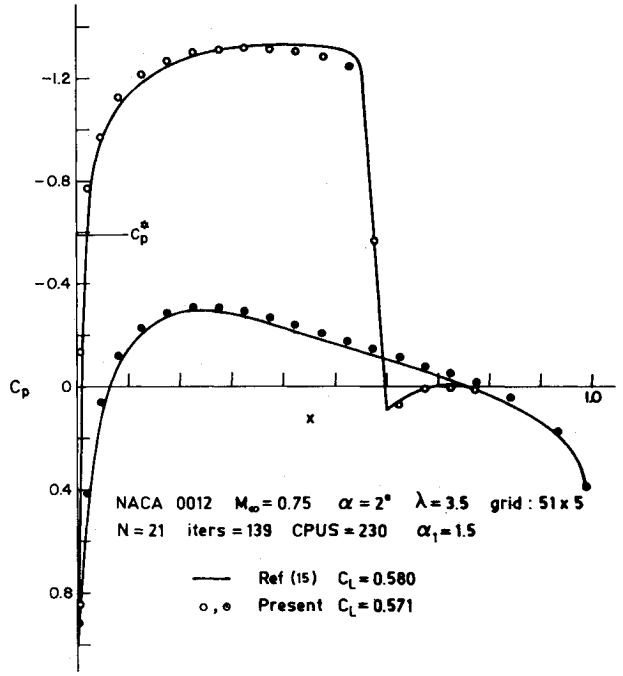

Fig. 7 Supercritical pressure distribution over NACA 0012 airfoil at incidence.

discrepancy between the two results near the trailing edge. This may be due to the fact that in Lock's case the airfoil is extended slightly beyond $x=1.0$ so as to close it, while in the present computations no such modification to the profile was made.

For both the above subcritical examples, converged solutions were obtained in about 10 iterations. The lifting case converged in about the same number of iterations as the symmetric case. This is in contrast to other calculation procedures where, because of the manner in which the Kutta condition is satisfied at the trailing edge at every iteration, the lifting case usually takes a larger number of iterations to converge than does the symmetric case.

Figure 6 shows the effect of the artificial viscosity parameter λ on the surface pressure distribution for symmetric flow past the NACA 0012 airfoil at $M_\infty=0.82$ and $\alpha=0$ deg. The symbol + in front of the figure in the column "iters" for $\lambda=2.6$ indicates that convergence for this case was obtained starting with the initial solution as the one obtained for $\lambda=3.0$. The figure shows that the peak velocities attained just ahead of the shock increase as the value of λ decreases, whereas the shock location itself remains fixed. At $\lambda=2.4$, the incipient peaky region ahead of the shock was accompanied by instability in the iteration scheme, which was terminated at 100 iterations. Thus, solutions differing significantly in the shock region, but agreeing broadly elsewhere, are obtainable depending upon the value of λ chosen. Such arbitrariness appears to be associated with other inviscid potential flow formulations as well[19] and is the result of the need to introduce artificial viscosity in the numerical scheme. The criterion adopted here for an appropriate choice of λ is that, from among a sequence of solutions for decreasing values of λ, the solution accepted does not show a peaky velocity profile just ahead of the shock and corresponds to the lowest value of λ.

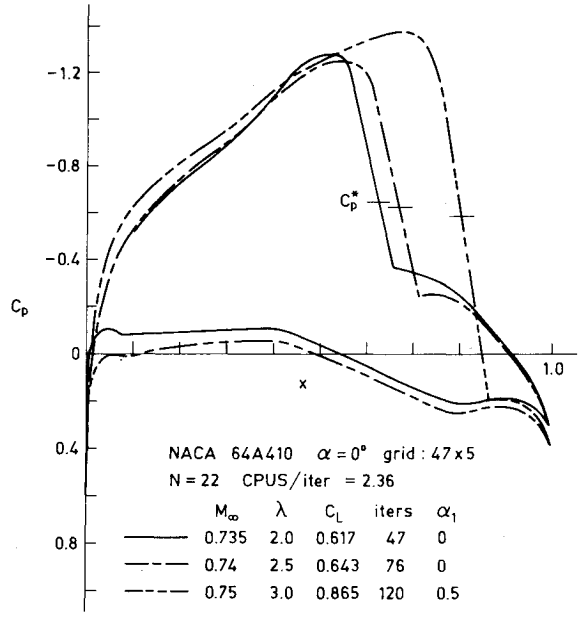

Fig. 8 Supercritical pressure distributions over NACA 64A410 airfoil at different freestream Mach numbers.

Figure 7 shows an example of supercritical lifting calculation. The computed surface pressure distribution for the NACA 0012 airfoil at $M_\infty=0.75$, $\alpha=2$ deg, and $\lambda=3.5$ is compared with the quasiconservative results of Bauer et al.[18] The agreement for this case is seen to be rather good, with the calculated lift coefficient being about 2% less than its value from finite difference calculations. Convergence for this case could be obtained only with the use of an artificial time-dependent term $\alpha_l u_t$ with $\alpha_l=1.5$. Also, attempts to obtain converged solutions for $\lambda<3.5$ for this case failed with or without the use of the artificial time-dependent terms.

Figure 8 shows the calculated surface pressure distribution for a NACA 64A410 airfoil at $M_\infty=0.735$, 0.74, and 0.75 and $\alpha=0$ deg. The rapid increase in the extent of the supersonic region and the strength of the shock with the increase in freestream Mach number is clearly evident. The capability of the present scheme to produce converged solutions for the strong supercritical case, $M_\infty=0.75$, with the supersonic region covering nearly 70% of the airfoil chord is clearly demonstrated. For this case, a value of $\alpha_l=0.5$ was also used to obtain convergence. The maximum local Mach number reached for this case was about 1.4. This is higher than the generally accepted value of 1.3 as the upper limit of validity of the weak shock assumption.

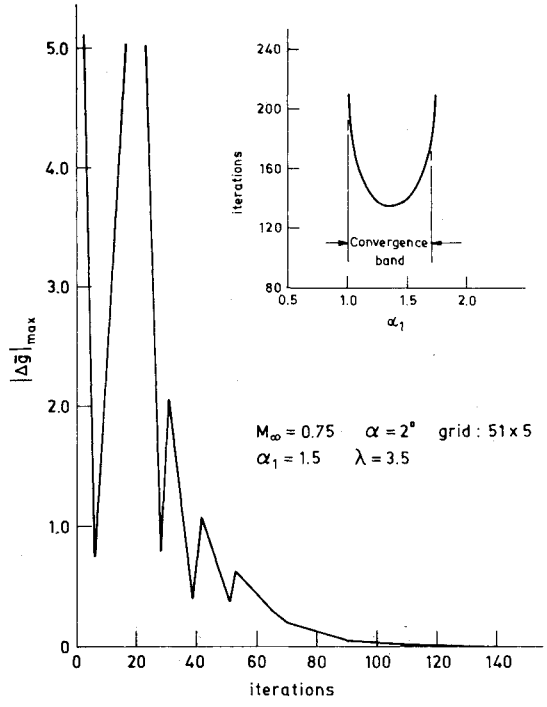

Fig. 9 Convergence history for supercritical flow past NACA 0012 airfoil and effect of α_1 on convergence.

Figure 9 shows a plot of the incremental change $\max_{i,j} |\Delta \bar{g}|$ against the iteration count for the test case shown in Fig. 7. The inset plots the parameter α_1 against the number of iterations required for convergence. Convergence for this case could be achieved only in a narrow band of α_1 values of 1.0-1.75.

V. Conclusions

The integral equation method has been successfully employed to compute supercritical solutions of the two-dimensional full potential equation satisfying exact tangency boundary conditions. The present method combines the influence coefficient method with elements of the finite difference methods to achieve reduction in storage requirements (which otherwise for the integral equation method could be rather large) and computing time without affecting the accuracy of the final results. For supercritical flows, the method is able to capture reasonably sharp shocks spread over just two to three mesh widths, whose strengths and locations agree well with the quasiconservative results of finite difference calculations. The present approach shows that the use of an incompressible linear operator with the addition of artificial viscosity to the governing equation is sufficient to produce convergence for most cases arising in inviscid isentropic flows with shocks. This is in contrast to the semidirect methods based on finite differences where the use of a Poisson-type iterative scheme without the use of artificial time damping terms leads to divergence for even slightly supercritical flows.[19] Convergence performance of the method in general has been found to be satisfactory and the iteration counts are rather small.

The method involves the computation of a large number of influence coefficients and their storage, although fortunately it gives good results even with grids that are very coarse compared to the finite difference grids. The second drawback of the method is that, in its present formulation, it is restricted to flows with only subsonic freestream Mach numbers. Also, the use of the point singularities in the internal singularity model robs the method of some of the flexibility that is desirable in choosing the collocation points and the computational grid, although for the cases so far computed, the model as presented here has worked satisfactorily. However, it is prehaps desirable and possible to dispense with these point singularities and represent the internal singularity distributions by continuous functions.

Acknowledgments

This work was supported by the Aeronautics (R&D) Board, Ministry of Defence, Government of India. The first author acknowledges the research assistantship made available to him under the grant-in-aid scheme of the ARDB.

References

[1] Jameson, A., "Transonic Flow Calculations," *Numerical Methods in Fluid Dynamics*, edited by H. J. Wirz and J. J. Smolderen, Hemisphere Publishing Corp., New York, 1978, Chap. 1.

[2] Holst, T., "Implicit Algorithm for the Conservative Transonic Full-Potential Equation Using an Arbitrary Mesh," *AIAA Journal*, Vol. 17, Oct. 1979, pp. 1038-1045.

[3] Holst, T., "Fast Conservative Algorithm for Solving the Transonic Full-Potential Equation," *AIAA Journal*, Vol. 18, Dec. 1980, pp. 1431-1439.

[4] Caughey, D. A. and Jameson, A., "Progress in Finite Volume Calculations for Wing-Fuselage Combinations," *AIAA Journal*, Vol. 18, Nov. 1980, pp. 1281-1288.

[5] Eberle, A., "Transonic Flow Computations by Finite-Elements: Airfoil Optimization and Analysis," *Recent Developments in Theoretical and Experimental Fluid Mechanics*, edited by U. Muller, K. G. Roesner, and B. Schmidt, Springer-Verlag, New York and Berlin, 1979, pp. 249-256.

[6] Piers, W. J. and Sloof, J. W., "Calculation of Transonic Flow by Means of a Shock Capturing Field Panel Method," AIAA Paper 79-1459, 1979.

[7] Ravichandran, K. S., Arora, N. L., and Singh, R., "Axisymmetric Transonic Flow past Slender Bodies Including Perforated Wall Interference Effects," *AIAA Journal*, Vol. 20, Nov. 1982, pp. 1557-1564.

[8] Spreiter, J. R., "Transonic Aerodynamics—History and Statement of the Problem," *AIAA, Progress in Aeronautics and Astronautics: Transonic Aerodynamics*, Vol. 81, edited by D. Nixon, AIAA, New York, 1981, pp. 3-79.

[9] Luu, T. S., Goulmy, G., and Dulieu, A., "Calcul de l'e'coulement transsonique autour d'un profil en admettant la loi deo compressibilite exacte," paper presented at Association Technique Maritime et Aeronautique Session, 1972.

[10] Stricker, R., "On an Integral Equation Method for Calculation of the Fully Non-Linear Potential Flow about Arbitrary Section Shapes," paper presented at Euromech Colloquium 75 on the Calculation of Flow Fields by Means of Panel Methods, Rhode/Braunschweig, May 1976.

[11] Kraus, W., "Panel Methods in Aerodynamics," *Numerical Methods in Fluid Dynamics*, edited by H. J. Wirz and J. J. Smolderen, Hemisphere Publishing Corp., New York, 1979, Chap. 4.

[12] Lock, R. C., "Test Cases for Numerical Methods in Two Dimensional Transonic Flows," AGARD Rept. 575, 1970.

[13] Basu, B. C., "A Mean Camber Line Singularity Method for Two-Dimensional Steady and Oscillatory Aerofoils and Control Surfaces in Inviscid, Incompressible Flow," ARC CP 1391, Oct. 1976.

[14] Mercer, J. E., Geller, E. W., Johnson, M. L., and Jameson, A., "Transonic Flow Calculations for a Wing in a Wind Tunnel," *Journal of Aircraft*, Vol. 18, Sept. 1981, pp. 707-711.

[15] Jameson, A., "Iterative Solutions of Transonic Flows over Airfoils and Wings, including Flows at Mach 1," *Comm. Pure and Applied Mathematics*, Vol. 27, 1974, pp. 283-309.

[16] Hafez, M., South, J., and Murman, E., "Artificial Compressibility Methods for Numerical Solutions of Transonic Full-Potential Equation," *AIAA Journal*, Vol. 17, 1979, pp. 838-844.

[17] Hess, J. L. and Smith, A. M. O., "Calculation of Non-Lifting Potential Flow About Arbitrary Three-Dimensional Bodies," *Journal of Ship Research*, Vol. 8, No. 2, Sept. 1964, pp. 22-44.

[18] Bauer, F., Garabedian, P., Korn, D., and Jameson, A., "Supercritical Wing Sections II," *Lecture Notes in Economics and Mathematical Systems*, Vol. 108, Springer-Verlag, New York and Berlin, 1975.

[19] Martin, E. D. and Lomax, H., "Rapid Finite-Difference Computation of Subsonic and Transonic Aerodynamic Flows," *AIAA Journal*, Vol. 13, May 1975, pp. 579-586.